

# Slow interaction ramps in trapped many-particle systems: universal deviations from adiabaticity

Masudul Haque and F. E. Zimmer

Max Planck Institute for the Physics of Complex Systems, Nöthnitzer Str. 38, 01187 Dresden, Germany

For harmonic-trapped atomic systems, we report universal non-adiabatic features in the response to interaction ramps. We provide results for several different systems in one, two, and three dimensions: bosonic and fermionic Hubbard models realized through optical lattices, a Bose-Einstein condensate, a fermionic superfluid and a fermi liquid. The deviation from adiabaticity is characterized through the heating or excitation energy produced during the ramp. We find that the dependence of the heat on the ramp time is sensitive to the ramp protocol but has aspects unexpectedly common to all systems considered. We explain these common features in terms of universal dynamics of the system size or cloud radius.

**Introduction** — Adiabaticity is an essential and ubiquitous concept in quantum dynamics. In the current era of many novel non-equilibrium experimental possibilities, *deviations* from adiabaticity in slow parameter changes have attracted a lot of attention [1–10]. The question of non-adiabaticity is of fundamental interest, but also has practical implications. Many experimental protocols involve adiabatically changing a parameter in order to reach a desired quantum state. Since non-adiabatic heating can rarely be completely avoided, it is essential to understand deviations from adiabaticity in slow ramps. While the effect of quantum critical points in the ramp path has been considered in much detail [1, 2], settings for non-equilibrium experiments in isolated systems tend to be mesoscopic rather than macroscopic, without true quantum critical points. Understanding non-adiabatic ramps in *finite* quantum systems is therefore vital. Also, since cold atoms dominate experimental non-equilibrium studies, a harmonically trapped many-particle system is the most important paradigm today for studying quenches and ramps. A few studies of ramps in finite and trapped systems have appeared in the very recent literature [9, 10], indicating an emerging recognition of the importance of the adiabaticity issue in finite systems. In addition, in the past couple of years, reports of experimental investigations of finite-rate interaction ramps have started to appear, both in the continuum [11] and in optical-lattices [12–14], with harmonically trapped atoms.

In this work, we consider non-adiabatic ramps in several *distinct* interacting many-particle systems, confined in isotropic harmonic traps. In each case, we consider ramps of the interaction from an initial value  $U_i$  to a final value  $U_f$ , occurring in time scale  $\tau$ . We focus on large but finite  $\tau$  (near-adiabatic ramps). We study deviations from adiabaticity through the heating  $Q$ , which is the final energy at time  $t \gg \tau$  minus the ground state energy of the final Hamiltonian. This quantity is also called the residual energy or excess excitation energy [3–5, 9], and may be thought of as the “friction” due to imperfect adiabaticity [15]. The asymptotic form of  $Q(\tau)$  is a quantitative characterization of minimal corrections to adiabaticity. Ref. [14] reports measurements of excess energies after ramps, which may be regarded as the first experimental approach to this quantity.

We find that the asymptotics of  $Q(\tau)$  is common to all the compressible systems that we considered: we have thus un-

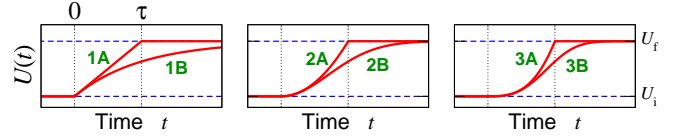


FIG. 1: Ramp shapes. We illustrate  $U_f > U_i$ ; it should be straightforward to visualize  $U_f < U_i$  cases.

covered *universal* non-adiabatic features of ramp dynamics in trapped systems. The  $Q(\tau)$  function has overall power-law decay,  $Q \sim \tau^{-\nu}$ , with the exponent  $\nu$  depending on the shape of the ramp. For certain ramp shapes,  $Q(\tau)$  has oscillations superposed on top of the power-law decay. We present results for a range of systems, interactions, and dimensionalities, which make clear that the universal features are independent of system details and generally do not depend on the initial and final values of the interaction, as long as the trapped system remains in the same phase.

Since the effects are universal over a wide range of trapped systems, they should be due to some type of dynamics that is prevalent in many harmonically trapped systems. We show that the relevant dynamics is the size oscillation or breathing-mode oscillation of the trapped cloud. Almost all trapped systems have “soft” breathing modes due to vanishing density at the edge, irrespective of the nature of intrinsic modes of the system. Our results show that, in the slow ramp limit, the breathing modes due to trapping dominate the near-adiabatic response of many systems. To show that the asymptotic behaviors of  $Q(\tau)$  are due to size dynamics, we will use a variational description for one of the systems (the Bose condensate), treating the extent (radius) of the many-particle cloud as a time-dependent variational parameter. Such a “radius dynamics” description will be shown to reproduce the universal  $Q(\tau)$  behaviors in thorough detail. An equivalent formulation is not easy to set up for all the systems; nevertheless, the commonality of the  $Q(\tau)$  features, and the success of the radius description for at least one case, is convincing argument that the same dynamics type is the relevant feature in each case.

Trapped atoms are by far the most promising setup for experimentally exploring isolated-system dynamics in general and non-adiabaticity issues in particular. A universal excitation mechanism that is dominant in generic trapped systems is thus an important baseline perspective for understanding

the many further non-adiabatic ramp experiments expected in the near future. Contemporary theoretical treatments of non-adiabaticity in many-particle systems almost invariably appeal to cold-atom experiments for motivation. Yet, our results show that in a real trapped-atom experiment radius dynamics dominates over the intrinsic heating mechanisms that may be important in individual uniform systems.

*Distinct trapped systems* — We will present results for fermionic and bosonic systems, with and without optical lattices. The lattice systems are two-component fermions, and single-component bosons, described respectively by the fermionic and bosonic Hubbard models:

$$H_{fH} = - \sum_{\langle ij \rangle \sigma} \left( c_{i\sigma}^\dagger c_{j\sigma} + h.c. \right) + U \sum_j n_{j\uparrow} n_{j\downarrow} + H^{\text{tr}} ;$$

$$H_{bH} = - \sum_{\langle ij \rangle} \left( b_i^\dagger b_j + h.c. \right) + U \sum_j n_j (n_j - 1) + H^{\text{tr}} .$$

We use the (inverse) hopping strength as energy (time) units; the notations are otherwise standard. In one dimension (1D), the trap terms are  $H^{\text{tr}} = \frac{1}{2} k_{\text{tr}} \sum_j j^2 c_{j\sigma}^\dagger c_{j\sigma}$  for fermions and  $\frac{1}{2} k_{\text{tr}} \sum_j j^2 b_j^\dagger b_j$  for bosons. We will consider both spin-balanced ( $N_\uparrow = N_\downarrow$ ) and polarized ( $N_\uparrow \neq N_\downarrow$ ) fermionic systems. We treat time evolution of the lattice systems through exact numerical evolution of the full quantum wavefunction, for few-particle configurations in 1D. The Bose-Hubbard model is also treated via the Gutzwiller approximation, for  $N > 10$  bosons and/or for 2D.

The continuum systems (without optical lattice) are the Bose-Einstein condensate (BEC) and the interacting two-component Fermi gas. We use trap units for these cases, expressing lengths (energies) in units of trap oscillator length (trapping frequency). The BEC is treated via the Gross-Pitaevskii (GP) description [16, 17]. The dynamics is given by the time-dependent GP equation,  $i \frac{\partial \psi}{\partial t} = -\frac{1}{2} \nabla^2 \psi + \frac{1}{2} r^2 \psi + U(t) |\psi|^2 \psi$ , and the GP energy functional is

$$E[\psi] = \int_r \left[ -\frac{1}{2} \psi^* \nabla^2 \psi + \frac{1}{2} U(t) |\psi|^4 + \frac{1}{2} r^2 |\psi|^2 \right] .$$

Here  $r$  is the radial position;  $\int_r \equiv \int d^D r$  is the spatial integral for dimensionality  $D$ ;  $U$  is the effective interaction strength whose relation to the physical interaction is also  $D$ -dependent (c.f. Ref. [18] for 1D). We normalize  $\int_r |\psi|^2 = 1$ , so that  $U$  contains a factor of the boson number  $N$ ; thus  $U$  can be large even within the mean-field regime. We will present GP results general to all  $D$ .

In addition to full solutions of the GP equation, we also use a variational description which uses the radius or size of the condensate,  $\sigma(t)$ , as the time-dependent parameter. Using a gaussian ansatz for the cloud shape, the equation of motion for  $\sigma$  is found to be

$$\sigma \sigma'' + \sigma^2 - \sigma^{-2} - (\sqrt{2\pi} \sigma)^{-D} U(t) = 0 , \quad (1)$$

the primes denoting time derivatives. The energy is

$$E[\sigma] = \frac{1}{4} D [\sigma^{-2} + \sigma^2 + (\sigma')^2] + \frac{1}{2} (\sqrt{2\pi} \sigma)^{-D} U(t) . \quad (2)$$

This radius description is suitable for describing breathing-mode oscillations. For constant  $U$ , for small-amplitude oscillatory solutions  $\sigma = R_0 + \rho \sin(\Omega t)$  (amplitude  $\rho$ ), Eq. (2) shows that the excitation energy scales as  $\sim \rho^2$ . We could also use a Thomas-Fermi instead of Gaussian profile; the results are very similar and do not affect our arguments.

Finally, the continuum fermionic system (3D) will be treated in the hydrodynamic approximation. There are several similar formulations; we choose the so-called “time-dependent DFT” [19], where the fermi gas is described by a nonlinear Schrödinger equation,  $i \frac{\partial \psi}{\partial t} = [-\frac{1}{2} \nabla^2 + \frac{1}{2} r^2 + \mu(n, U)] \psi$ . Here  $n = |\psi|^2$  is the sum of the (equal) densities of the two components. We use the Hartree expression:  $\mu(n, U) = \frac{1}{2} (3\pi^2 n)^{2/3} + \frac{1}{2} U n$ . Both a paired superfluid ( $U < 0$ ) and a Fermi liquid ( $U > 0$ ) are described by the same formalism. Analogous to the BEC case, we use a variational description to formulate the dynamics in terms of the cloud radius.

*Ramp shapes* — We analyze ramps of the form

$$U(t) = U_i + \theta(t) (U_f - U_i) s(t/\tau) .$$

The ramp function  $s(x)$  starts at  $s(0) = 0$  and ends at  $s(\infty) = 1$ . The ramps take place over time scale  $\tau$  but we do not require them to end at  $t = \tau$ . (Contrast, e.g., Ref. [4].) We choose a collection of ramps which allows us to compare the presence/absence of kinks and various exponents. Specifically, we consider the following forms for  $s(x)$ :

|      |                                 |      |                |
|------|---------------------------------|------|----------------|
| [1A] | $x \theta(1-x) + \theta(x-1)$   | [1B] | $1 - e^{-x}$   |
| [2A] | $x^2 \theta(1-x) + \theta(x-1)$ | [2B] | $1 - e^{-x^2}$ |
| [3A] | $x^3 \theta(1-x) + \theta(x-1)$ | [3B] | $1 - e^{-x^3}$ |

Each [A], [B] pair has the same initial behavior,  $s(x) \sim x^\alpha$ , but the [B] versions have no endpoint kinks (Fig. 1).

*Universal features of ramp response* — In Fig. 2 we present the behavior of the heat function  $Q(\tau)$ , normalized against its instantaneous-quench value  $Q(\tau = 0)$ . The small- $\tau$  behavior and the exact magnitude of  $Q(\tau)$  are system- and approximation-dependent; the universal features we present concern only the asymptotics of  $Q(\tau)/Q(0)$ .

In the left panels, the  $Q(\tau)$  behaviors are compared for the ramp shapes  $s(x) \sim x^\alpha$  with discontinuous derivatives at endpoints, [1A], [2A], [3A]. Each curve has an overall power-law decay with the same decay exponent,  $Q(\tau) \sim \tau^{-2}$ . This suggests that the residual energy for such ramps is primarily set by the endpoint kink. Superposed on the power-law decay are oscillations, which are often but not always smaller for larger  $\alpha$  (contrast panels (c) with others). The oscillation strength decays faster for larger  $\alpha$ , as  $\tau^{-2\alpha}$ .

The right panels concern smoothed ramps [1B], [2B], [3B], which lead to non-oscillating decay of  $Q(\tau)$ . The decay exponent is seen to depend on the power  $\alpha$  of  $s(x) \sim x^\alpha$ , namely,  $Q(\tau) \sim \tau^{-2\alpha}$ .

The dimensionality does not affect the decay exponents or general behavior. As an example, results are shown for the

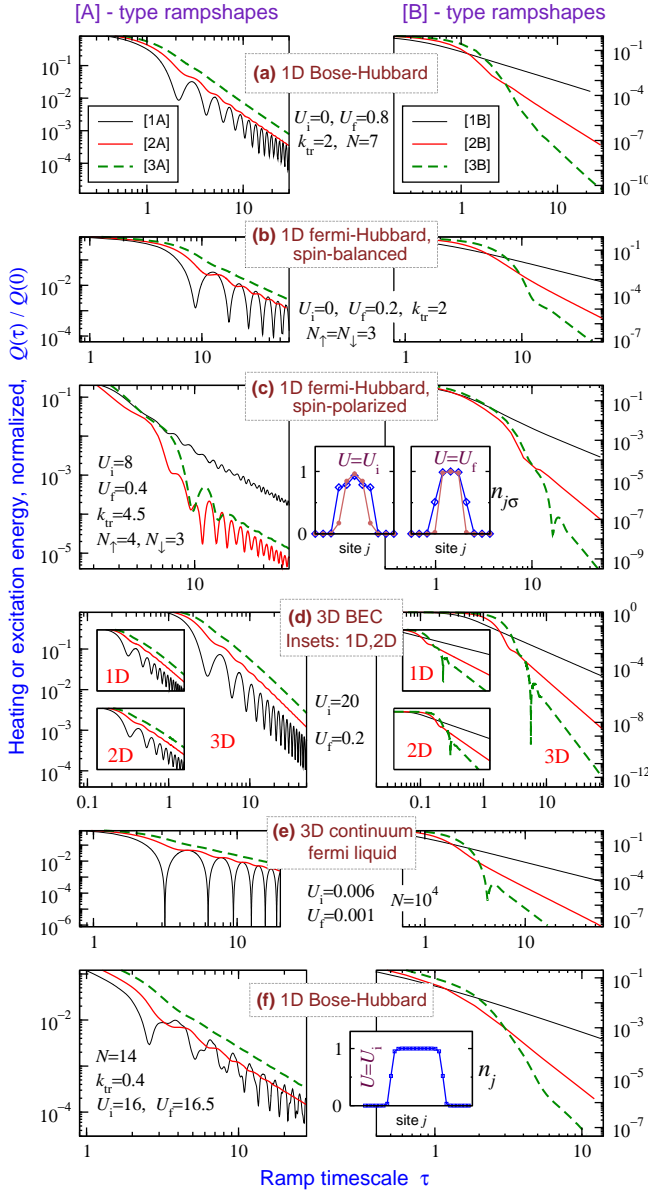


FIG. 2: The normalized excitation energy or heat,  $Q(\tau)/Q(0)$ , for various trapped systems.  $(U_i, U_f)$  values and trap constants  $k_{tr}$  are chosen over a wide range to emphasize the parameter-independence of the effects. Response to [A] ramps (left panels) shows overall  $Q(\tau) \sim \tau^{-2}$  decay, with superposed oscillations that decay faster for larger- $\alpha$  ramps. For [B] ramps (right panels) the asymptotic behavior is pure  $\tau^{-2\alpha}$  decay. Insets to (c): density profiles for  $U = U_{i,f}$  ground states. For (f),  $U = U_{i,f}$  ground-state profiles are very similar, only  $U_i$  shown.

BEC in 1D, 2D, and 3D, in the (d) panels and insets. We have also found that the same exponents and oscillation features also appear in additional cases not shown, e.g., a continuum Fermi superfluid (3D,  $U < 0$ ), the Bose-Hubbard model in higher  $D$  (treated via the Gutzwiller approximation), etc.

The (c) and (f) panels involve systems which cannot be described as having single-radius profiles. The two spin components have different extents in the spin-imbalanced Hub-

bard model (c); the Bose-Hubbard situation (f) has superfluid wings around a Mott core. The  $Q(\tau)$  behaviors are more rich for these systems; however, the features discussed above remarkably also persist in these more complex cases.

*Radius dynamics interpretation* — We now show how radius dynamics explains the  $Q(\tau)$  behaviors presented above. We will use the convenient formulation of BEC radius dynamics, Eqs. (1) and (2). Fig. 3 (top row) shows the radius of a 2D BEC evolving as a function of time for various ramp shapes, for reasonably large  $\tau$ . In the center and bottom rows, we show the deviation of  $\sigma(t)$  from the equilibrium radius corresponding to the instantaneous value of the interaction,  $R_0(t) = R_0[U(t)]$ . For a truly adiabatic ramp,  $\sigma(t)$  would follow  $R_0(t)$  exactly; therefore the deviation  $f(t) = \sigma(t) - R_0(t)$  is at the heart of non-adiabaticity and this quantity determines the heating  $Q$ . After the ramp, the  $f(t)$  function is purely oscillatory;  $Q$  scales as the square of the oscillation magnitude. The oscillations initiated at the beginning of the ramp are of magnitude  $\mathcal{O}(\tau^{-\alpha})$  for the  $(t/\tau)^\alpha$  ramp. In the case of [A] ramps (middle row), the endpoint kink causes an  $\mathcal{O}(\tau^{-1})$  oscillation, which is parametrically larger for  $\alpha > 1$  and hence dominates the final dynamics, leading to overall  $Q(\tau) \sim \tau^{-2}$  behavior.

We first explain the  $\sim \tau^{-1}$  scaling of oscillations initiated at the kink. If we neglect the smaller oscillations at  $t < \tau$ , the radius  $\sigma(t) \approx R_0(t)$  at the kink  $t = \tau$  has “correct” value for  $U = U_f$ , i.e.  $f$  is negligible. However the derivative is nonzero,  $\sigma'(t) \approx R'_0(t)|_{t=\tau}$ , which scales as  $\sim \tau^{-1}$ . Thus we have the following “initial” conditions at  $t = \tau^+$  for subsequent evolution:  $f(\tau) = 0$ ,  $f'(\tau^+) = c_0 \tau^{-1}$ . Using  $f(t > \tau) \approx \rho \sin(\Omega t + \delta)$ , these initial values imply  $\rho \sim \tau^{-1}$ . This explains the  $\mathcal{O}(\tau^{-1})$  oscillation magnitude of  $f(t > \tau)$ , and hence  $\mathcal{O}(\tau^{-2})$  heating, for ramps having an endpoint kink.

The oscillations of  $Q(\tau)$  (Fig. 2 left panels) can be explained by relaxing the approximation  $f(t < \tau) \approx 0$  made above. The small oscillations of  $f(t < \tau)$  guarantee that  $\sigma'(t = \tau)$  oscillates around  $R'_0(t = \tau)$  as a function of  $\tau$ . This causes final breathing mode amplitude  $\rho$  to oscillate around its  $\mathcal{O}(\tau^{-1})$  value as a function of  $\tau$ . The  $f(t < \tau)$  oscillation strength is  $\mathcal{O}(\tau^{-\alpha})$  (shown below); hence the  $Q(\tau)$  oscillations decay as  $\tau^{-2\alpha}$ , as seen in Fig. 2 left panels.

For smooth [B] ramps (Fig. 3 bottom), the breathing-mode strength ( $\sim \tau^{-\alpha}$ ) initiated at the beginning of the ramp remains unchanged; there is no kink to abruptly create larger oscillations. We therefore need only to explain the strength of oscillations at the beginning of the ramp, where  $s(t/\tau) \approx (t/\tau)^\alpha$ . For this, we rewrite Eq. (1) as an equation for  $f(t)$ . For simplicity, we will write this out explicitly only in the limit  $U_{i,f} \gg 1$ , and small oscillations,  $f(t) \ll R_0(t)$ . (The arguments can of course be modified to go beyond the large- $U$  restriction. Small  $f(t)$  is guaranteed for large  $\tau$ .) We obtain

$$f''(t) + \Omega^2 f(t) + \frac{u''(t)}{(D+2)u^{\frac{D+1}{D+2}}} - \frac{(D+1)u'(t)^2}{(D+2)^2 u^{\frac{2D+3}{D+2}}} = 0, \quad (3)$$



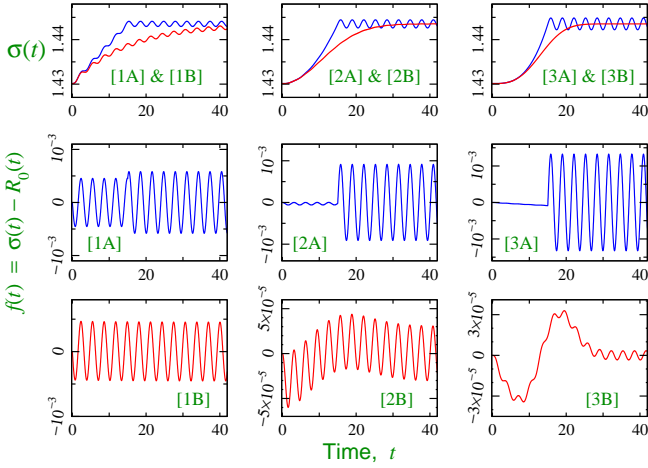


FIG. 3: Top row: radius dynamics  $\sigma(t)$  for various ramp shapes,  $\tau = 15$ . Center and bottom rows: deviation  $f(t)$  from the ‘instantaneous’ ground-state radius  $R_0(t)$ . 2D BEC;  $(U_i, U_f) = (20, 21)$ .

with  $u = U/(2\pi)^{D/2}$ . The first two terms give pure oscillations (breathing mode at fixed  $u$ ); the last two terms are corrections due to time-varying interaction. We first treat  $\alpha > 1$  ramps. The initial conditions at  $t = 0^+$  are then  $f(0) = f'(0) = 0$ . With  $u = u_i + (\delta u)(t/\tau)^\alpha$ , the  $u''$  correction is dominant compared to the  $u'^2$  correction at  $t \ll \tau$ . The dominant correction terms take the form  $c_1/\tau^2$  for  $\alpha = 2$ , and  $c_1 t/\tau^3$  for  $\alpha = 3$ . The solutions of the resulting differential equation are sums of oscillatory and algebraic terms. It is straightforward to verify that the boundary conditions  $f(0) = f'(0) = 0$  force the oscillatory part to have coefficients scaling as  $\sim \tau^{-\alpha}$ . This explains the  $Q \sim \tau^{-2\alpha}$  behavior for integer  $\alpha > 1$ . The  $\alpha = 1$  case is slightly different. The initial condition still involves  $\sigma'(0) = 0$ , but since  $R_0(t) = [u(t)]^{1/(D+1)}$  has finite slope at  $t = 0^+$ , this now corresponds to  $f'(0^+) = -R'_0(0^+) = -c_3/\tau$ . This initial condition leads to a purely oscillatory  $f(t)$  with amplitude  $\sim \tau^{-1}$ , which explains  $Q(\tau) \sim \tau^{-2}$  for  $\alpha = 1$ .

*Discussion; Open questions* — Considering various harmonic-trapped atomic clouds, we have presented results on the adiabaticity question, demonstrating universal aspects in the first corrections to adiabatic behavior for slow ramps. We have shown that the slow-ramp response is determined by the radius-oscillation modes common to many trapped atomic systems, and its exact form depends on the ramp shape. We have explained the universal effects using a single-radius description of the cloud. This covers a wide range of interesting systems, but it is even more remarkable that our universal features extend to at least some systems which cannot be described by a single radius.

We have shown that a final kink in the ramp shape plays a drastic role in the non-adiabatic response of compressible trapped systems. A recently discovered effect of such kinks is logarithmic contributions to  $Q(\tau)$  [2, 4, 7]. The effect we have found for trapped systems (kink induces larger oscillations overwhelming initial excitation) is quite different.

Our work opens up several new research avenues. Like other “universal” results, it is important to identify the limits of validity. For example, do the same  $Q(\tau)$  asymptotic features appear in trapped systems not described by a single radius? Paradigm examples are Bose-Hubbard systems containing superfluid-insulator “wedding-cake” structures, and phase-separated imbalanced Fermi gases near unitarity. We have shown some examples where the same behaviors appear [Figs. 2(c,f)], but a general understanding is lacking. It is likely that the dynamics of one radius-like variable generally dominates the extreme asymptotics, recovering our results.

Each of the systems are of intense interest in their own right, and understanding less universal features in parameter quenches is important for the individual systems, especially with growing experimental interest and capabilities for studying ramps and quenches. Ramps in the trapping frequency should also induce radius oscillations, but details might be different from interaction ramps. The case of anisotropic harmonic traps also remains an open issue. One might speculate that one of the trapping frequencies dominate the extreme asymptotics, but the intermediate- $\tau$  region might show interesting interplay of the several frequencies and associated radii.

- 
- [1] See review and citations of earlier work in: J. Dziarmaga, Adv. Phys. **59**, 1063 (2010); A. Polkovnikov, K. Sengupta, A. Silva, M. Vengalattore, Rev. Mod. Phys. **83**, 863 (2011).
  - [2] C. De Grandi, V. Gritsev, and A. Polkovnikov, Phys. Rev. B **81**, 012303 (2010); **81**, 224301 (2010).
  - [3] T. Caneva, R. Fazio, and G. E. Santoro, Phys. Rev. B **76**, 144427 (2007). F. Pellegrini, S. Montangero, G. E. Santoro, and R. Fazio, Phys. Rev. B **77**, 140404(R) (2008). T. Caneva, R. Fazio, and G. E. Santoro, Phys. Rev. B **78**, 104426 (2008).
  - [4] M. Eckstein and M. Kollar, New J. Phys. **12**, 055012 (2010).
  - [5] E. Canovi, D. Rossini, R. Fazio, and G. E. Santoro, J. Stat. Mech. (2009) P03038.
  - [6] M. Moeckel and S. Kehrein, New J. Phys. **12**, 055016 (2010).
  - [7] B. Dóra, M. Haque, and G. Zaránd, Phys. Rev. Lett. **106**, 156406 (2011).
  - [8] J. Dziarmaga and M. Tylutki, arXiv:1109.3801.
  - [9] T. Venumadhav, M. Haque, and R. Moessner, Phys. Rev. B **81**, 054305 (2010).
  - [10] G. Roux, Phys. Rev. A **81**, 053604 (2010). J.-S. Bernier, G. Roux, and C. Kollath, Phys. Rev. Lett. **106**, 200601 (2011). M. Collura and D. Karevski, Phys. Rev. Lett. **104**, 200601 (2010). S. Natu, K. Hazzard, and E. Mueller, Phys. Rev. Lett. **106**, 125301 (2011).
  - [11] N. Navon, S. Piatecki, K. J. Günter, B. Rem, T. C. Nguyen, F. Chevy, W. Krauth, and C. Salomon, arXiv:1103.4449.
  - [12] C. Hung, X. Zhang, N. Gemelke, and C. Chin, Phys. Rev. Lett. **104**, 160403 (2010).
  - [13] W. S. Bakr *et al.*, Science **329**, 547 (2010).
  - [14] D. Chen, M. White, C. Borries, and B. DeMarco, Phys. Rev. Lett. **106**, 235304 (2011).
  - [15] J. G. Muga, Xi Chen, A. Ruschhaupt, and D. Guery-Odelin, J. Phys. B **42**, 241001 (2009). A. del Campo, Phys. Rev. A **84**, 031606(R) (2011).
  - [16] L. P. Pitaevskii, Sov. Phys. JETP **13**, 451 (1961).

- [17] E. P. Gross, *Nuovo Cimento* **20**, 454 (1961).
  - [18] M. Olshanii, *Phys. Rev. Lett.* **81**, 938 (1998).
  - [19] Y. E. Kim and A. I. Zubarev, *Phys. Rev. A* **70**, 033612 (2004).
- S. K. Adhikari, *Phys. Rev. A* **77**, 045602 (2008).